Cerebral Biophoton Emission as a Potential Factor in Non-Local Human-Machine Interaction

Joey M. Caswell*, Blake T. Dotta†, Michael A. Persinger*†

ABSTRACT

Subjects were instructed to employ intention to affect the direction of random number generation from a device located on their right side at 1 m distance. Biophoton emissions from the right hemisphere were recorded simultaneously. Significant increases (~$3.5 \cdot 10^{-12}$ $W \cdot m^{-2}$) in photon radiant flux density occurred when there were marked deviations from random variations suggesting that the correlative variable for intent was coupled to cerebral photon emission. Cross-spectral analyses indicated a significant coupling between photon density and deviation from random variation within the 6 mHz range. The estimated raw power over the most likely area of influence (10^{-10} m^2) over the peak duration would be within the order of 10^{-20} J. This quantum is associated with single action potentials and the difference in energy equivalents after Lorentz contraction between the electron's Compton wavelength and traditional particle width. The resulting ~1.5 µm wavelength for this energy, which matches Bohr's solution, is also within the width of the synapse. The moderately strong correlation between the strength of the coherence between the deviations during intention and the photon emission and the entropy within the temporal distribution of the "random" number variations in the mHz range suggests that a shared source with the earth's free background oscillations may be involved. Our results strongly indicate that photon-electron interactions between cerebral function and electronic devices that reflect "random" electron tunnelling may be more powerful than accommodated by classical physics and indicate the powerful role of a neuroquantological process.

Key Words: consciousness, random event generator, photons, non-local, intention

DOI Number: 10.14704/nq.2014.12.1.713 **NeuroQuantology 2014; 1: 1-11**

Introduction

Photons are the quanta of electromagnetic radiation, essentially particles of light. Their average energies, according to the relationship $E = h \cdot c \cdot \lambda^{-1}$, are typically within the range of 10^{-19} J for the ultraviolet to infrared portions of the electromagnetic spectrum. Although traditionally thought to possess no mass, recent evidence has suggested a non-zero rest mass for the photon (upper limit ~10^{-52} kg; Tu *et al.*, 2005). The phenomenon of biophoton emission (BPE) refers to the occurrence of ultraweak light emission from biological matter, typically in association with reactive oxygen species formation and cellular metabolism (Apel & Hirt, 2004). Biophotons have been a major focus in the area of biophysics for a number of years (e.g., Li *et al.*, 1983; Chang, 2008), and novel approaches to molecular biology have been revealed through the study of this mechanism (e.g., Isojima *et al.*,

Corresponding author: Michael A. Persinger
Address: Consciousness and Neuroquantum Research Laboratory, Human Development Program* and Biomolecular Sciences Program†, Laurentian University, Sudbury, Ontario Canada.
e-mail ✉ mpersinger@laurentian.ca
Relevant conflicts of interest/financial disclosures: The authors declare that the research was conducted in the absence of any commercial or financial relationships that could be construed as a potential conflict of interest.
Received: Sept 30, 2013; **Revised:** Nov 22, 2013;
Accepted: Jan 6, 2014

1995; Gourley *et al.,* 2005). Subsequent experiments have suggested the plasma membrane of the cell as the most likely source (Dotta *et al.,* 2011). BPE has also been examined in the context of the human body (e.g., Kobayashi *et al.,* 2009). Furthermore, this phenomenon has been suggested as a potential mechanism in cellular communication (Sun *et al.,* 2010). A number of more exotic applications have been proposed in this area.

Bokkon's innovative theories (2005; 2009) have implicated biophotons in visual imagery. In order to test this hypothesis, recent experiments examined the relationship between BPE, visualization, as well as intention, which suggest that imagining white light consistently produces an increase in photon emission from the right side of the head compared to both mundane thoughts and baseline conditions (Dotta & Persinger, 2011). The radiant flux density associated with BPE increases was measured to be approximately $5{\cdot}10^{-11}$ W·m^{-2} and was estimated to be associated with ~10^7 cortical neurons (Dotta *et al.,* 2012). It was subsequently revealed that BPE was significantly and strongly correlated with electroencephalographic (EEG) power during this task. Aside from the more obvious relationship with visual imagery revealed by these studies, cerebral biophotons have also been suggested as a potential mechanism in consciousness (Amoroso, 1999; Dotta *et al.,* 2013). Furthering Bokkon's hypotheses, studies have revealed properties of photon entanglement (e.g., Persinger & Lavallee, 2010) and the potential transfer of non-local information (Dotta & Persinger, 2009) in the context of human brain activity and cerebral biophotons.

Given the apparent associations between consciousness, intention, biophotons, and non-locality, it is suggested that cerebral BPE may play a role in mediating non-local physical anomalies associated with consciousness. Although evidence supporting this contention has been examined in the context of *incoming* non-local information (Persinger & Saroka, 2012), BPE has not been studied during processes associated with *outgoing* non-local information. The phenomenon of consciousness-correlated collapse (3C) has suggested that a human operator is capable of influencing the outcome of a non-deterministic external system through mental intention alone (e.g., Jahn *et al.,* 1997; Radin & Nelson, 2003). Although brain activity has been examined to some degree during this apparent interaction (Gissurarson, 1992), the non-local qualities of photon emissions and their intimate link to consciousness provide a reasonable measure of potential influence within 3C processes. The following experiment tested the hypothesis that BPE may be a factor involved in the apparent influence of cognitive "intention" on an external random physical system. We measured BPE from the right side of participants' heads while they focused their intention on a random event generator (REG) device in order to produce a desired outcome in the data. It was hypothesized that specific ranges of photon emission would be associated with various levels of overall performance, determined by the overall magnitude of deviation within the REG data, as well as specific ranges of individual events. It was further speculated that any relationship between photon emission and REG device output would likely become apparent upon examination of both spectral characteristics of the data and statistical signal complexity.

Methods

Subjects

Participant age ranged from 22-42 years for N = 11 (N = 8 females, N = 3 males). All were recruited from Laurentian University campus.

Equipment

Biophoton emission (BPE) for the first N = 8 participants was measured using a Model 15 Photometer from SRI Instruments (Pacific Photometric Instruments), which contained a unit scale ranging in single units from 1 to 100. Calibration indicated a single unit was equal to ~$5{\cdot}10^{-11}$ W·m^{-2}. The photomultiplier tube (PMT) housing (BCA IP21) for the RCA electron tube was placed at a distance of approximately 15 cm from the right side of the participant's head. Data output was sent to a laptop computer with a sampling rate of 3 samples per second. Participants in this test segment contributed n = 23 individual sessions. BPE for the latter N = 3 participants was obtained using a digital photometer Model DM009C (Senstech Ltd.), also placed ~15 cm from the right side of the head, with a sample rate of 50 samples per second. This measured the numbers of individual photons in each sample as opposed to an absolute measure of power. Values from all trials were subsequently averaged and

standardized accordingly. Data obtained from both PMT models were compared in previous experiments which revealed congruence between the devices (e.g., Persinger *et al.,* 2013). Participants in this segment contributed n = 4 individual sessions.

Random data was produced using a Psyleron REG-1 random event generator (Figure-1; www.psyleron.com). The device produces a random output which is generated by electron tunneling effects within two field effect transistors. The varying voltage levels which result from this process are converted into digital data through a gated sampling procedure which allows for regularly spaced bit sequences. The output of both transistors is internally compared through an alternating (0, 1) XOR masking process in order to maintain true randomness and reduce any potential influence of physical artefacts or other external environmental variables (Jahn *et al.,* 2000). The device itself is further protected from static electromagnetic factors by an aluminum outer shielding and a Permalloy mu-metal inner shield. Furthermore, the device was rigorously calibrated prior to shipment in order to ensure output conformed to statistical expectations. The random event generator (REG) was also tested in control experiments within our laboratory to confirm these expectations. The resulting data stream is collected through USB-port using Psyleron FieldREG and Reflector software packages on a laptop computer. Data was produced at a rate of 2 events (200 0,1 bits/event) per second, with each event referring to the number of 1's out of 200 bits with binary probabilities, represented by a value of 0-200. The theoretical (chance) mean for each event is 100 with a standard deviation of √50.

Measures of entropy (HX) were computed using Matlab 2011a software. All other statistical procedures, including spectral analyses, were conducted using SPSS software v.17.

Procedure

Prior to testing, participants viewed a short demonstration with the REG software (e.g., Figure-2) in order to understand upon what they would be focusing their intention. No feedback was provided during testing. They were seated in a dark, comfortable environment, approximately 1 m away from the REG (right side, placed on a wooden table 14.5° below the horizontal plane of the temporal lobes). The PMT was located 15 cm from the right side of the head (Figure-3). They were then asked to intend for the data output of the REG to deviate either up or down for one to three periods of ~8 minutes each while the PMT measured photon emission. REG software data collection was hidden from the experimenters during this process.

Figure 1. Random event generator (REG); Psyleron REG-1 device used throughout the following experiment.

Figure 2. Screenshot of Reflector software collecting data from REG device; jagged center line is the moving cumulative deviation.

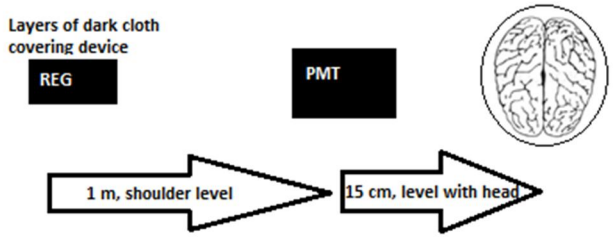

Figure 3. Schematic of experiment; relative positions of REG, PMT, and human operator.

Results

Data Transformation

Random Event Generator (REG) data was collected for a total of 27 test sessions from N = 11 participants. Individual REG event scores were standardized according to .5 chance expectations using z-scores ([*x*-100] /√50). Overall session scores were obtained using Stouffer's method (∑*z*/√n), where *z* = individual event z-scores, with n = the number of events. While participants intended for a specific outcome in the REG data biophoton emission was recorded from the right side of the head with a photomultiplier tube (PMT). One model of PMT was used for N = 8 participants (23 sessions), while a second model was used for N = 3 participants (4 sessions). In order to accommodate varied sampling across PMTs, as well as individual differences, all photon data was standardized independently within each session using z-scores. Prior to transformation each session was de-trended by entering PMT data into a linear regression with time as the independent variable and obtaining the residual values for subsequent standardization and analyses. Mean values and standard deviations were computed for each minute (8) of both REG and PMT data. All sessions were used as separate trials (N = 27).

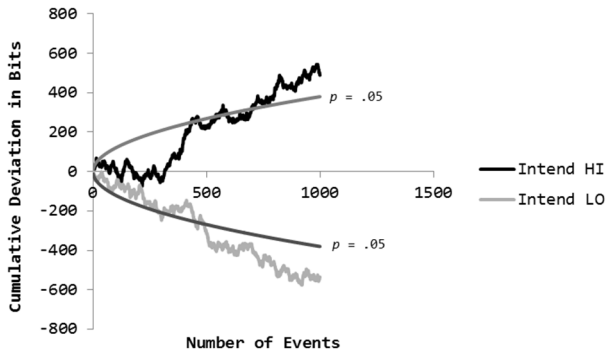

Figure 4. Cumulative deviations for two sessions with the greatest overall deviations, both in the intended direction (actual directionality of data maintained); parabolas indicate threshold for statistical significance (p = .05, one-tailed).

Investigating Session Serial Position

Out of the N = 11 participants involved in this experiment there were N = 8 who each completed three consecutive sessions. Each session consisted of an identical number of individual events (n = 1000), and therefore unweighted Stouffer's z-scores were adequate for comparing results between sessions. Overall session z-scores were converted to directional measures with regard to operator intention (e.g., output deviated in intended direction = positive value). One-way analysis of variance (ANOVA) indicated that there were no statistically significant differences between sessions 1, 2 or 3 (p>.05). The two largest individual deviations (z > 2), both in the intended direction, were obtained within sessions 1 and 3 (Figure-4).

Differences in Photon Emission between REG Session Scores

Data was entered into a cluster analysis which grouped trials by overall session REG score. Three clusters emerged that represented positive deviations, negative deviations, and deviations which closely approximated chance expectation results. A one-way analysis of variance (ANOVA) was then performed to determine potential differences in photon emission between REG score using three clusters (Tables 1 & 2). There was a significant difference revealed between clusters for the mean photon emission during minute 2 (Figure-5; $F_{(2, 26)} = 4.18$, $p = .03$, $\eta^2 = .26$). Post-hoc tests (Tukey) found a significant difference between clusters 1 and 3 (p = .022), but not clusters 1 and 2 (p = .82), or 2 and 3 (p = .08). This timeframe (2 minutes) is precisely what we had previously found (Caswell *et al.,* 2013) for potential gravitational, electromagnetic, and cerebral effects involved in this phenomenon. Furthermore, when data were examined using a temporal resolution of seconds (Figure-6), there were significant increases in PMT units associated with individual REG events at both high and low extremes of ordered deviation (F = 8.41, p = .005, η^2 = .13). The mean and standard deviations for the analog PMT units were 40 and 1.03, respectively. For a z-score increase of 0.07 (Figure 6) the net increases in flux density would have been $3.5 \cdot 10^{-12}$ W·m^{-2}.

Table 1. N, μ (mean) and *sd* (standard deviation) values of actual REG session scores for each cluster.

Cluster	N	μ (REG)	*sd* (REG)
1	14	-.038	.523
2	9	1.505	.401
3	4	-1.79	.407

Spectral Characteristics

Spectral analysis is a statistical method used in signal processing which allows examination of a

random time-series with respect to the frequency domain as opposed to time. This process is used to decompose a particular signal into simpler components, and is particularly useful given that many signals or processes may be described as the summation of a number of individual frequencies. Spectral power density is obtained for a number of frequencies up to the Nyquist limit (n/2) for a time series.

Table 2. N, μ (mean) and *sd* (standard deviation) values of average (minute 2) PMT z-scores for each cluster.

Cluster	N	μ (PMT)	*sd* (PMT)
1	14	-.098	.255
2	9	-.03	.283
3	4	.329	.229

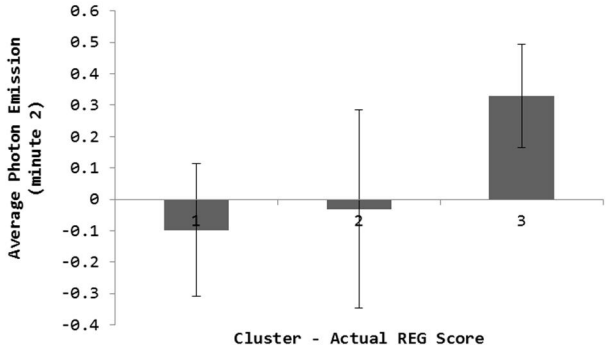

Figure 5. Difference in average photon emission during minute 2 between actual REG session score clusters; vertical bars are standard deviations (*sd*).

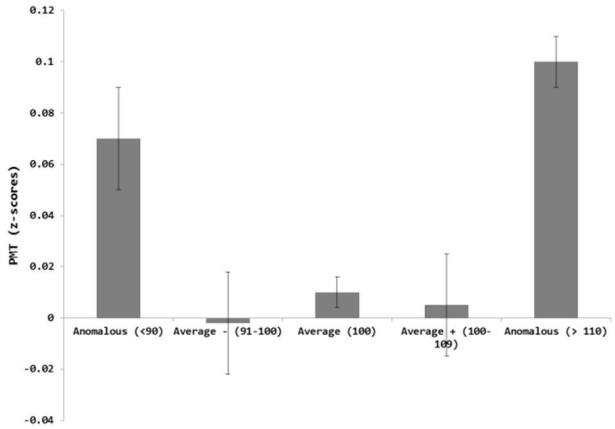

Figure 6. Difference in standardized PMT units associated with specific ranges of REG event scores (each event = sum of 200 0, 1 bits); Anomalous (<90), Average - (91-100), Average (100), Average + (100-109), Anomalous (>110); vertical bars represent standard error of the mean (SEM).

Spectral density itself is a measure of power within a signal after it has been decomposed into separate frequencies following Fourier transform (Figure-7).

In this example, there is an apparent spike in PMT spectral power density during significant REG operations compared to non-significant events which occurs at a frequency of .272 Hz (3.68 s). Although subtle the effect was consistent within individual records. The difference in PMT spectral power density between a significant and non-significant REG session for a single participant is shown in Figure 8. A number of quantifiable processes associated with each spectral frequency of a given signal can be obtained through this process, including phase, amplitude, and power. We have found that z-scores of the raw data from which a spectral power density is derived will minimize the inflation effects from the absolute values of the numbers that compose the scale.

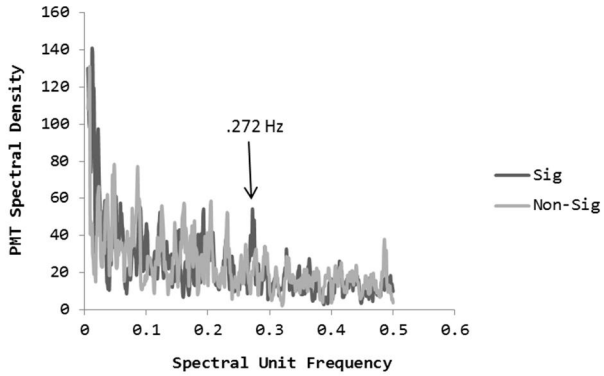

Figure 7. Power spectrum of photon emission during significant (Sig) and non-significant (Non-Sig) REG output for a single participant using complete samples (n = 1000). The results are derived from 1 s sampling increments. This pattern was also noted in other participants during the course of the study.

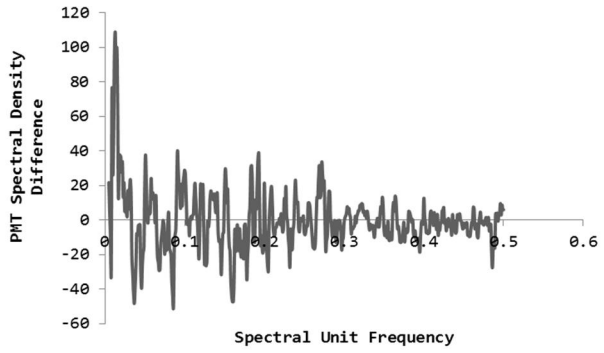

Figure 8. Difference in PMT spectral power density between a significant and non-significant REG session for a single participant (Spectral density significant – Spectral density non-significant), 1 s increments.

A bivariate or cross-spectral analysis can be employed to obtain a number of statistics associated with the spectral densities of two random variables, including the amplitude of their cross-spectral densities (Figure-9), which is a measure of the difference between the extreme values of the variables examined. The cross-spectral coherence is also typically used. This value refers to the covariance observed between the spectral power densities of two variables within each frequency (Figure-10). REG and PMT data were each transformed to 10 second averages for each test session and entered into a series of separate cross-spectral analyses.

Averages of 10 seconds were employed in order to diminish any temporal "mismatching" between the devices; because both devices were manually controlled it is possible that the output of REG and PMT data could have been discrepant by ~1-2 seconds. The averaging procedure was used in order to better align the output between devices. Furthermore, this reduction in individual data points also resulted in fewer frequency bands for subsequent analyses. This amounted to n = 50 points for REG and PMT data from each session, which subsequently resulted in 25 frequency bands. Data was transposed in order to examine relevant values of each frequency in isolation. Actual frequencies were computed by dividing 1 by the spectral unit frequency multiplied by the unit of time (e.g., spectral unit frequency of .28 = (1 /.28) · 10 s = 35.7 s). Dividing 1 by the real frequency in seconds yields a value in Hz (.28 = 1 / 35.7 = 28 mHz). For comparison this is within the range of slow electrical processes ("infraslow" potentials) within the brain (Aladjalova, 1964).

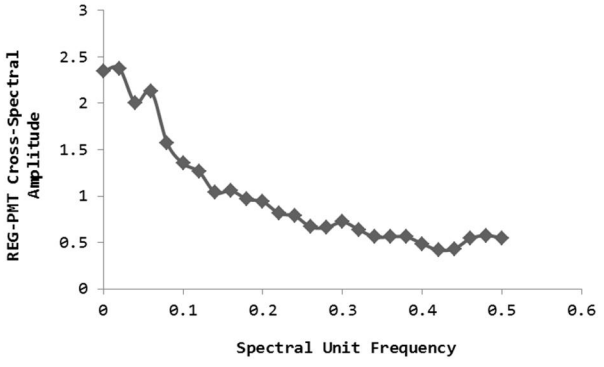

Figure 9. Amplitude of REG and PMT cross-spectra averaged across all sessions for each frequency, 10 s averages.

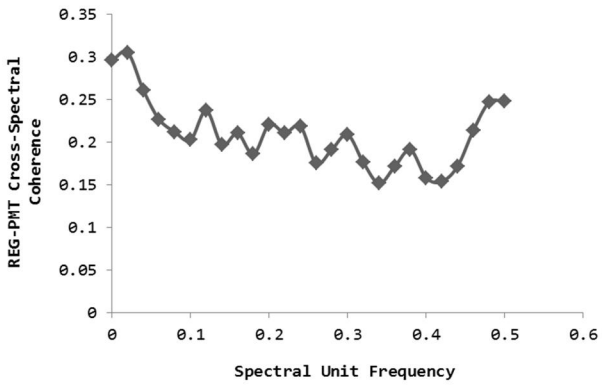

Figure 10. Cross-spectral coherence (covariance) observed between REG and PMT spectral densities averaged across all sessions for each frequency, 10 s averages.

Cross-spectral amplitude between REG output and PMT measures was entered into a number of parametric and non-parametric correlational analyses with overall REG session scores. Only those of $p < .05$ and $r \geq .5$ are reported. It was determined that the values for cross-spectral amplitude corresponding to a frequency of 28 mHz were significantly correlated with the actual value of REG session scores (Figure- 11; $r = -.58$, $p = .002$; *rho* = -.505, $p = .007$). This suggests that the magnitude of the difference between the extreme values of REG output and PMT measures were statistically related to the final overall value obtained by the REG device. More specifically, as the photon flux density from the brain diminished the REG effect increased.

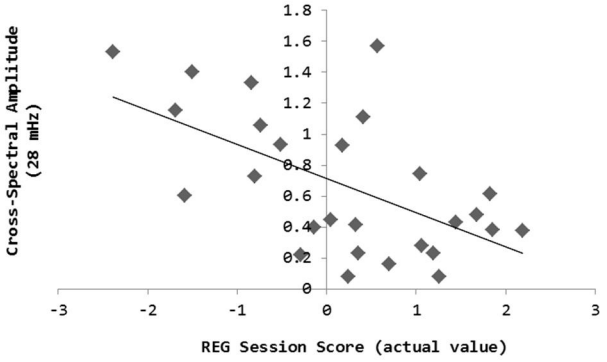

Figure 11. Correlation between cross-spectral amplitude (28 mHz) and overall REG session score (actual value).

Signal Complexity

Entropy as applied to information theory is generally used to describe the measure of uncertainty or predictability within a random variable (Jaynes, 1957). The application of entropy to statistical prediction was originally

formulated by Shannon (1948), and follows the basic equation for Shannon entropy $H(X) = -\sum_x P(x)\log_2 P(x)$, where x = the random variable, X = the number of possible values within x, and *P* = the probability mass function. The entropy function in the Matlab software package was used to obtain a value similar to the Shannon entropy for a time series using an internal algorithm. A base 2 logarithm was employed in order to produce values in units of bits. Variables with a greater number of distinct values, as well as those within which these values are more evenly distributed possess greater statistical entropy. Therefore, higher values for entropy (HX) indicate greater complexity, while low values represent greater predictability within the signal.

Using the entropy function, HX values were computed for all individual REG sessions and examined for correlations with cross-spectral properties obtained in the previous analysis. Pearson and Spearman analyses revealed a significant correlation between HX values of REG data (e.g., the overall complexity) and the cross-spectral coherence corresponding to a frequency of 6 mHz (Figure-12; r = -.543, *rho* = -.55, p = .003). This suggests that the overall statistical complexity of REG results is related to the covariance observed between spectral power density of REG and PMT measures within the 6 mHz frequency. More specifically as the coherence between the REG and photon emission data within this discrete band of the earth's continuous free oscillations (Nishida *et al.,* 2000) decreased the complexity of the information increased.

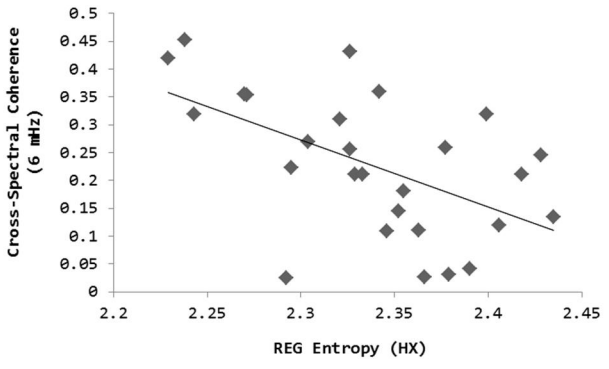

Figure 12. Correlation between REG entropy values (HX) and cross-spectral coherence (6 mHz).

A cluster analysis was performed using HX values of each sample. Three clusters were chosen for further analysis of variance (Tables 3 & 4) based on previous results using three groups of REG z-scores. This method revealed statistically significant differences in the PMT standard deviation during minute 3 of testing (Figure-13; $F_{(2, 26)}$ = 4.051, p = .03, η^2 = .253). Post-hoc tests (Tukey) indicated a significant difference between clusters 1 and 2 (p = .028), but not 1 and 3 (p = .197) or 2 and 3 (p = .637). This would suggest that the average departure from the mean of photon emission in minute 3 significantly differed between participant clusters based on overall complexity of REG output.

Table 3. N, μ (mean) and sd (standard deviation) values of REG entropy scores for each cluster.

Cluster	N	μ (HX)	sd (HX)
1	11	2.342	.016
2	8	2.404	.022
3	8	2.268	.028

Table 4. N, μ (mean) and sd (standard deviation) values of minute 3 PMT standard deviations (z-scores) for each cluster.

Cluster	N	μ (PMT)	sd (PMT)
1	11	.752	.264
2	8	1.02	.14
3	8	.925	.173

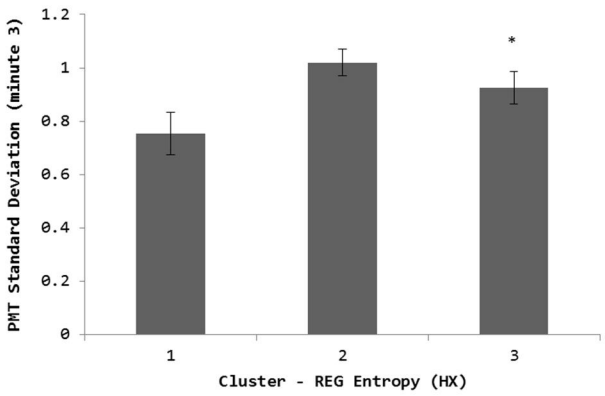

Figure 13. Difference in PMT standard deviation during minute 3 between REG entropy clusters; vertical bars represent standard error of the mean (SEM); * indicates a non-significant difference from cluster 1 (p > .05).

Discussion

There has been a long history of experimentation and speculation that the physical presence of a human being or the engagement in cognitive activity near dynamic processes can affect their consequences. For decades research and casual observation have indicated that "intention" can affect objects in

motion. More specifically these objects display a transient acceleration (Jahn *et al.,* 2000). With the growing presence of electronic devices within the human environment, the contribution of the physical bases of "intention" to their operations has become evident. Although the energy levels, as Bohr anticipated, would be very small, they would be within the order of magnitude associated with the bifurcation in events where one direction or another occurs. The increment of energy associated with a single shift from one electron shell to another could result in a cascade that ultimately influences the current structure of matter at macrolevels.

The results of the present study replicated the multiple experimental observations that normal people who are proximal to random number generators can significantly affect the deviations of the intrinsic dynamic processes within these devices. In addition, we have shown that the deviations are associated with measurable, physical changes within the brains of the participants. These changes involved the emissions of biophotons from the cerebral volume as measured by photomultiplier tubes. Comparable effects were measured from both digital and analogue equipment; hence, the phenomena were not likely to be a consequence of idiosyncratic instrumentation.

The primary relationship between the increased quantitative measures (radiant flux density) of photon emissions from the right cerebrums of the participants and deviations of random number generation from "chance variation" occurred for both extremes. Periods of enhanced photon flux density from the right hemisphere were associated with both positive and negative extremes of the REG score. The observation was more reflective of a scalar process analogous to the long history of "psi hitting" and "psi missing" that has confounded paranormal researchers for decades.

The reliable increase in a specific power density associated with the extreme deviations from chance variation in REG scores could indicate the source. The increase in power density increase was $\sim 3.5 \cdot 10^{-12}$ $W \cdot m^{-2}$. If we assume the likely focus of the effect would involve the approximate width of an average (10 μm) neuronal soma (which is within range of p-n junctions) the power is $3.5 \cdot 10^{-22}$ $J \cdot s^{-1}$ (W) and when distributed over the duration of 6 mHz, which showed the strongest coherence between the extreme REG deviations and photon power densities, the energy is within the order of 10^{-20} J.

A *NeuroQuantum unit* of $\sim 2 \cdot 10^{-20}$ J (Persinger, 2010) is the energy associated with influence of an action potential ($\Delta v = 1.1 \cdot 10^{-1}$ V) upon a unit charge ($1.6 \cdot 10^{-19}$ A·s). The action potential is considered the primary correlate of the fundamental dynamic process within the human cerebrum that mediates intention and cognition. If thought is to be coupled to influence upon random number generation then the congruence between the energy associated with the physical substrate of intention and the photon emissions that could affect electron tunnelling within the REG devices would be expected. From a more popular perspective, the energy associated with thought and intention would be transferred into a particular range of probabilities for electron tunnelling.

The two solutions for the length of an electron, the Compton λ ($2.42 \cdot 10^{-12}$ m) and the classical ($2.1 \cdot 10^{-15}$ m) values, would require a specific value to be accommodated by the Lorentz contraction. The difference in velocities approaching c, the velocity of light in a vacuum, that would be required to produce this discrepancy in distance that defines the wave vs the particle properties of an electron results in a discrete quantum. This value is $\sim 10^{-20}$ J. This could be the quantity of energy associated with the frequently hypothesized "collapse of the wave" function attributed to consciousness and intention (Dotta and Persinger, 2009).

There is a second implication for this congruence. The spin energy for s=1/2 spin quantum number that reflects normal matter can be calculated as $S = \hbar \cdot 2\pi\sqrt{(s(s+1)}$, where ħ is modified Planck's constant. The solution is $1.055 \cdot 10^{-34}$ J·s multiplied by 0.866, or $0.914 \cdot 10^{-34}$ J·s. When divided by the energy associated with an average action potential, the frequency is $1.95 \cdot 10^{14}$ Hz. Assuming the velocity of light in a vacuum, the equivalent wavelength would be 1.54 μm.

This solution is quite salient. Bohr (see Lewis, 1921) showed that the quantum for removing or adding a nucleus from a neutral hydrogen molecule (consisting of two similar nuclei each carrying a unit charge with two electrons rotating in a ring between the nuclei) could be calculated from the equation $f = 1.32 \cdot \dot{\omega}_o \sqrt{(m \cdot M^{-1})}$, where m is the mass of the electron

and M is the mass of the proton. With the latter ratio of 1835 and $\acute{\omega}_o$=1.91·10^{14} Hz, the equivalent wavelength (λ)=1.57 μm. This width is also within the upper range of the width of a synapse or the width of a node of Ranvier within the human cerebral cortices. Although this convergence does not prove the origin from the synapse or along the axon barrel, the similarities suggest a direction for future exploration.

In fact, if we assume the spin for photons=1, then the quantum energy is 1.492·10^{-34} J·s and the equivalent wavelength would be 2.23 μm. The difference between the derived photon spin wavelength and that associated with matter (1.54 μm) is 690 nm, which is within the visible range. For traditional models such differences could reflect phase relationships. If this explanation is accurate, then future experiments that compare photon emissions from the brains of participants through filters for this wavelength should demonstrate the greatest proportion of the effect compared to adjacent wavelengths.

The relevance of 6 mHz is more germane when the contributory role of the earth's free background oscillations is considered. They display a range between 2 and 7 mHz (Nishada *et al.,* 2000). Specific windows, 3.7 mHz and 4.3 mHz, reveal coupling between the Earth's surface vibrations (Raleigh waves) and atmospheric acoustic oscillations. The typical amplitude for this range of oscillations is 0.5·10^{-11} m·s^{-2}. We (Persinger, 2012) have found that daily power of spectral density in background photon emissions from the ground in our basement laboratory within the 3 mHz range, the one that couples ground and atmospheric oscillations, displays seasonal variations similar to the acoustic oscillations described by Nishada et al (2000).

The product of the 1.5 kg of brain mass and this acceleration is 0.7·10^{-11} N and when applied over the 0.1 m length of the cerebrum would be 7·10^{-13} J. For 6 mHz (the coherence peak in our data), the equivalent power would be 4.2·10^{-15} W. The spectral power density over the cross sectional area of the right temporal lobe (~2.5·10^{-3} m^2) would be the equivalent of ~1.7·10^{-12} W·m^{-2}. This quantity is within the error of measurement of the power density increase recorded during the most extreme deviations from random variation recorded by the REG.

There are several interpretations for this complex relationship. At present we are assuming that the greater coherence at ~6 mHz between the photon flux density from the right hemisphere and the deviations for the REG in conjunction with less complexity in the variation of the numbers generated "spontaneously" could reflect the effect of "intention". We are pursuing the idea that the biophotons are affecting the properties, particularly spin, within the REG devices that in term affect "random"; that is, the process exerts a biological signature of some small order. The congruence between the estimated energies that would be available to the cerebral mass from this band of the Earth's free oscillations and those measured during our experiments may be a source of variance that could explain some of the variability between experiments in various laboratories as well as seasonal or daily differences.

Increased standard deviations in the measurements for one group compared to another often reflect the introduction of another source of variance within the former. The appearance of a resonance factor within a spectrum can produce this effect. The increased variability of photon flux density from the right hemisphere during the third minute in conjunction with increased entropy (complexity) score in the REG, the opposite of the 6 mHz relationship, could explain why these processes are "self-limiting". It may be relevant that the occurrence of the greatest increased entropy during the third minute (120 to 180 s) is the equivalent of between 5.5 and 8 mHz. This range encompasses the major extent of the free background oscillations displayed by the earth.

The photon measurements in the present study were obtained 15 cm from the skull along the right side. Assuming a radius of ~5.5 cm from the center of the brain, then the energy over this surface area of the sphere with a radius of 20.5 cm is 5.23·10^{-1} m^2 · 3.5·10^{-12} W·m^{-2} or 1.8·10^{-12} J·s^{-1} during the extreme deviations in the REG. This assumes no directionality. However, from the cerebral surface (3.8·10^{-2} m^{-2}), assuming a reverse inverse square relation, could have been as high as 2·10^{-11} J·s^{-1}. If non-locality rather than locality (some form of influence by propagation of photons to the REG 1 m away) were operating, then a comparable quantity of energy equivalence should emerge within the triggering circuitry.

We suggest a low probability explanation. The energy equivalence of an electron is ~$8.1 \cdot 10^{-14}$ J. The photon energy emitted from the cerebrum directly in our experiments could have been as high as $2 \cdot 10^{-11}$ $J \cdot s^{-1}$ or the equivalent of 240 "electrons". A routine calculation of REG bit rates indicates that every 1 s is associated with 400 bits. There is a requirement of 202 bits in one direction per s, more precisely the cumulative effect of 2,020 bits in one direction over 100 s, to obtain a significant z-score (p=.025).

Within 100 s and certainly 167 s (6 mHz), which would produce even more significant variations if the ratio of bits in one direction was maintained, there would be sufficient "transformation" of photon energies from the brain to electron "equivalences" to produce the effect. If this concept is even partially valid, then the role of thought-related photons upon the manifestation of virtual particles ("virtual electrons") to real particles that affect dynamics within Casimir-like settings as well as the degree by which these transformations determine causality must be reconsidered.

There were other periodicities shared by variations in the photon flux density from the brains of the participants and the REG data. The 28 mHz peak that was apparent across all sessions is equivalent to a period of about 36 seconds, or about two oscillations per minute. This duration is within the range of short-term memory when the electrical processes associated with representation of memory and the "stream of consciousness" rapidly decline. One would expect the fundamental energies from which intention emerges to utilize the "visual scratchpad" for short-term "storage" of information. The cerebral locus is primarily within the right hemisphere, particularly the right prefrontal region.

This range of periodicities is also the defining feature of the brain's "steady potentials" or infraslow potentials. This largely forgotten legacy from Aladjalova (1964), involves transcerebral electrical variations in the order of 0.3 to 1.5 mV with periods of 7 to 8 s and periods of 0.2 to 2 min. For reference, 0.5 mV is the increment of postsynaptic change over the membrane in response to the release of molecules from a single pre-synaptic vesicle, i.e., the miniature EPSP (excitatory postsynaptic potential). Rhythmic oscillations between 0.5 and 2 oscillations per second within amplitudes between 0.5 and 1.5 mV can occur for hours to days. They often follow periods of "stress" as well as marked memory consolidation. The role of glial cells, that constitute a syncytium of integrated connection throughout the cerebral volume, cannot be ignored. The resting membrane potential of astrocytes changes within about 4 to 6 sec following the electrical stimulation from neurons. The spectral peak for photon emission during REG outputs that deviated significantly from change compared to those that did not was ~4 s.

To our knowledge this is the first experiment to demonstrate a quantitative relationship between the deviation from random fluctuations in an electronic device and the photon emissions from cerebral function. We (Dotta *et al.,* 2012) had previously demonstrated that "imagining" (a type of intention) compared to mundane (passive or non-intention) thinking was associated with conspicuous and reversible photon emission from the right hemisphere that was strongly correlated with left prefrontal brain activity.

The coupling between electron-photon activity within the neuronal membrane, the presumed bases for the effect, and the electrons within the REG might still be reciprocal. The time required for a photon moving at c to traverse a 10 nm membrane is 10^{-16} s. This is the same order of magnitude as the time required for an electron to complete one orbit in a Bohr magneton. Consequently the "information" or some feature of "state" per unit orbit could be reversibly transferred as this dynamic photon traverses the neuronal cell membrane.

References

Aladjavlova NA. Slow electrical processes in the brain. Progress in Brain Res 1964, 7, 1-238

Amoroso RL. An introduction to noetic field theory: The quantization of mind. Noetic J 1999; 2(1): 28-37.

Apel K, Hirt H. Reactive oxygen species: Metabolism, oxidative stress, and signal transduction. Ann Rev Plant Biol 2004; 55: 373-399. http://dx.doi.org/10.1146/annurev.arplant.55.031903.141701

Bókkon I. Dreams and neuroholography: An interdisciplinary interpretation of development of homeotherm state in evolution. Sleep Hypno 2005; 7(2): 61-76.

Bokkon I. Visual perception and imagery: A new molecular hypothesis. BioSystems 2009; 96: 178-184. http://dx.doi.org/10.1016/j.biosystems.2009.01.005

Caswell JM, Collins MWG, Vares DAE, Juden-Kelly LM, Persinger MA. Gravitational and experimental electromagnetic contributions to cerebral effects upon deviations from random number variations generated by electron tunneling. Int Let Chem Phys Astro 2013; 11(2013): 72-85.

Chang JJ. Studies and Discussion of Properties of Biophotons and Their Functions. NeuroQuantology 2008; 6(4): 420-430. http://dx.doi.org/10.14704/nq.2008.6.4.198

Dotta BT, Koren SA, Persinger MA. Demonstration of entanglement of "pure" photon emissions at two locations that share specific configurations of magnetic fields: Implications for translocation of consciousness. J Consc Exp Res 2013; 4(1).

Dotta BT and Persinger MA. Dreams, time distortion, and the experience of future events: A relativistic, neuroquantal perspective. Sleep Hypno 2009; 11(2): 29-39.

Dotta BT and Persinger MA. Increased photon emissions from the right but not the left hemisphere while imagining white light in the dark: The potential connection between consciousness and cerebral light. J Consc Exp Res 2011; 2(10): 1463-1473.

Dotta BT, Buckner CA, Cameron D, Lafrenie RF, Persinger MA. Biophoton emissions from cell cultures: Biochemical evidence for the plasma membrane as the primary source. Gen Phys Biophys 2011; 30(3): 301-309.

Dotta BT, Saroka KS, Persinger MA. Increased photon emission from the head while imagining light in the dark is correlated with changes in electroencephalographic power: Support for Bokkon's biophoton hypothesis. Neuro Let 2012; 513: 151-154 http://dx.doi.org/10.1016/j.neulet.2012.02.021

Gissurarson LR. The psychokinesis effect: Geomagnetic influence, age and sex differences. J Sci Exp 1992; 6(2): 157-165.

Gourley PL, Hendricks JK, McDonald AE, Copeland RG, Barrett KE, Gourley CR, Singh KK, Naviaux RK. Mitochondrial correlation microscopy and nanolaser spectroscopy: New tools for biophotonic detection of cancer in single cells. Tech Cancer Res Treat 2005; 4(6): 585-592.

Isojima Y, Isoshima T, Negai K, Kikuchi K, Nakagawa H. Ultraweak biochemiluminescence detected from rat hippocampal slices. NeuroReport 1995; 6: 658-660. http://dx.doi.org/10.1097/00001756-199503000-00018

Jahn RG, Dunne BJ, Nelson RD, Dobyns YH, Bradish GJ. Correlations of random binary sequences with pre-stated operator intention: A review of a 12-year program. J Sci Exp 1997; 11(3): 345-367.

Jahn R, Dunne B, Bradish G, Dobyns Y, Lettieri A, Nelson R, Mischo J, Boller E, Bosch H,Vaitl D, Houtkooper J, Walter B.Mind/machine interaction consortium: PortREG replication experiments. J Sci Exp 2000; 14(4): 499-555.

Jaynes ET. Information theory and statistical mechanics. Phys Rev 1957; 106(4): 620-630. http://dx.doi.org/10.1103/PhysRev.106.620

Kobayashi M, Kikuchi D, Okamura H. Imaging of ultraweak spontaneous photon emission from human body displaying diurnal rhythm. PLoS ONE 2009; 4(7). http://dx.doi.org/10.1371/journal.pone.0006256

Lewis WC. A system of physical chemistry. Vol. 3. Quantum Theory. Sir W. Ramsay and F. G. Donnan (eds). Longmans, Green Co. London, 1921.

Li KH, Popp FA, Nagl W, Klima H. Indications of optical coherence in biological systems and its possible significance. In H. Fröhlich & F. Kremer (Eds.), Coherent Excitations in Biological Systems (pp. 117-122), 1983. http://dx.doi.org/10.1007/978-3-642-69186-7_11

Nishida K, Kobayashi N, Fukao Y. Resonant oscillations between the solid earth and the atmosphere. Science 2000; 287: 2244-2246. http://dx.doi.org/10.1126/science.287.5461.2244

Persinger MA. 10-20 J as a neuromolecular quantum in medicinal chemistry: an alternative approach to myriad molecular pathways. Cur Med Chem 2010; 17: 3094-3098. http://dx.doi.org/10.2174/092986710791959701

Persinger MA and Lavallee CF. Theoretical and experimental evidence of macroscopic entanglement between human brain activity and photon emissions: Implications for quantum consciousness and future applications. J Consc Exp Res 2010; 1(7): 785-807.

Persinger MA and Saroka KS. Protracted parahippocampal activity associated with Sean Harribance. Int J Yoga 2012; 5: 145-150. http://dx.doi.org/10.4103/0973-6131.98238

Persinger MA, Dotta BT, Saroka KS. Bright light transmits through the brain: Measurement of photon emissions and frequency-dependent modulation of spectral electroencephalographic power. World J Neuro 2013; 3: 10-16. http://dx.doi.org/10.4236/wjns.2013.31002

Radin DI and Nelson RD. Meta-analysis of mind-matter interaction experiments: 1959-2000. In Healing, Intention, and Energy Medicine (pp. 39-48). London: Harcourt Health Sciences, 2003. http://dx.doi.org/10.1016/B978-0-443-07237-6.50009-7

Shannon CE. A mathematical theory of communication. Bell Sys Tech J 1948; 27: 379-423, 623-656.

Sun Y, Wang C, Dai J. Biophotons as neural communication signals demonstrated in situ biophoton autography. Photochem Photobio Sci 2010; 9(3): 315-322. http://dx.doi.org/10.1039/b9pp00125e

Tu LC, Luo J, Gillies GT. The mass of the photon. Rep Prog Phys 2005; 68(1). http://dx.doi.org/10.1088/0034-4885/68/1/R02